ON THE EXTENDED KNOTTED DISKS OF GALAXIES

Dennis Zaritsky[1,2] and Daniel Christlein[3,4,5]

ABSTRACT

The stellar disks of many spiral galaxies are twice as large as generally thought. We use archival data from the *Galaxy Evolution Explorer* mission to quantify the statistical properties of young stellar clusters in the outer, extended disks of a sample of 11 nearby galaxies. We find an excess of sources between 1.25 and 2 optical radii, R_{25}, for five of the galaxies, which statistically implies that at least a quarter of such galaxies have this cluster population (90% confidence level), and no significant statistical excess in the sample as a whole beyond $2R_{25}$, even though one galaxy (M83) individually shows such an excess. Although the excess is typically most pronounced for blue (FUV − NUV < 1, NUV < 25) sources, there is also an excess of sources with redder colors. Although from galaxy to galaxy the number of sources varies significantly, on average the galaxies with such sources have 75 ± 10 blue sources at radii between $1.25R_{25}$ and $2R_{25}$. In addition, the radial distribution is consistent with the extended dust emission observed in the far-IR and with the properties of Hα sources, assuming a constant cluster formation rate over the last few hundred megayears. All of these results suggest that the phenomenon of low-level star formation well outside the apparent optical edges of disks ($R \sim R_{25}$) is common and long lasting.

Key words: galaxies: evolution — galaxies: fundamental parameters — galaxies: spiral — galaxies: structure

1. INTRODUCTION

Simple questions about galaxies can be difficult to answer. For example, the question "How large are disk galaxies?" has many answers. One could cite results regarding the edges of optical disks (van der Kruit & Searle 1981), of the star formation threshold (Kennicutt 1989), of H I disks (Roberts & Haynes 1994), or of dark matter halos (Zaritsky et al. 1993). Even within each of those specific aspects of spiral galaxies there are ambiguities. For example, recent results have shown that the stellar disks are often not sharply truncated (Pohlen et al. 2002; Pohlen & Trujillo 2006), that star formation exists beyond the radius of the sharp decline in star formation rate (Ferguson et al. 1998; Thilker et al. 2005), and that the main ingredient for star formation, molecular gas, exists at large radii (Braine & Herpin 2004). The discovery of radially extended star formation in at least some spiral galaxies has implications for a range of topics, including the growth and development of disks, star formation in low-metallicity, low-density environments, and galactic dynamics. So far, the presentation of extended star formation, either as H II regions (Ferguson et al. 1998) or UV knots (Thilker et al. 2005; Bianchi et al. 2005; Gil de Paz et al. 2005), has focused on the discovery of the phenomenon, and as such has been presented in either individual galaxies or samples of two or three systems. A statistical study was presented by Boissier et al. (2007), but while it focuses on integrated luminosity to reach interesting results regarding the star formation threshold and initial mass function (IMF), it does not treat the star clusters separately. Is there any systematic behavior in extended disk star cluster formation that we can identify? In particular, what is the pervasiveness and radial extent of the phenomenon? We use this study to lay some groundwork for our kinematic and chemical abundance studies of outer-disk H II regions (Christlein & Zaritsky 2007a; D. Christlein & D. Zaritsky 2007b, in preparation; S. Herbert-Fort et al. 2007, in preparation).

We use archival data from the *Galaxy Evolution Explorer* (*GALEX*) mission to study the phenomenon of UV-selected knots in the outer regions ($R > R_{25}$) of galaxies. Because our goal is to determine statistical properties valid for disk galaxies as a class, we stack the data for a suitable sample of galaxies and examine the angular cross-correlation function between the UV knots and the parent galaxy. This study will then provide a measure of the excess number of UV knots in the vicinity of nearby galaxies, and therefore of the prevalence and radial range of the extended star formation. In § 2 we describe the data and our treatment of them. In § 3 we describe the cross-correlation results, and in § 4 we discuss some implications.

2. SAMPLE SELECTION AND *GALEX* DATA

We select our sample of face-on, well-resolved disk galaxies from the extensive catalog of *GALEX* galaxy observations published by Gil de Paz et al. (2006). To select face-on galaxies, we define the inclination using the ratio of the major (a) to minor (b) axes appropriate for projected circular disks and then select galaxies with an inferred inclination less than 45°. To select galaxies of large angular extent that still lie well within a single *GALEX* pointing, so that we obtain a reliable measurement of the background source density from the same image, we retain only those galaxies with $2' < a < 10'$. The semimajor axis is taken from the compilation of Gil de Paz et al. (2006) and refers to the optical radius R_{25}. Finally, to select disk galaxies we require $0 <$ T type ≤ 7, where "T type" characterizes morphology as described in the Third Reference Catalog of Bright Galaxies (de Vaucouleurs et al. 1991) and our criteria span morphological types Sa to Sd. These selection criteria result in a sample of 20 galaxies. We then require that both high-quality far-UV (FUV) and near-UV (NUV) data exist in the MAST archive at the Space Telescope Science Institute. Lastly, we reject NGC 1068 because of the highly nonuniform background in the image that has most likely variably affected source detection. We arrive at the final

[1] Steward Observatory, University of Arizona, Tucson, AZ 85721, USA.
[2] Center for Cosmology and Particle Physics, Department of Physics, New York University, New York, NY 10003, USA.
[3] Andes Fellow.
[4] Departamento de Astronomia, Universidad de Chile, Santiago, Chile; dzaritsky@as.arizona.edu.
[5] Department of Astronomy, Yale University, New Haven, CT 06520, USA; christlein@astro.yale.edu.

TABLE 1
Disk Galaxy Sample

Name	$2a$ (arcmin)	$2b$ (arcmin)	i (deg)	D (Mpc)	x_0 (pixels)	y_0 (pixels)	R_1 ($\times a$)	R_2 (pixels)
NGC 628	10.5	9.5	25.2	11	1933	1910	1.25	1300
NGC 1042	4.7	3.6	40.0	18	2336	1483	1.50	1300
NGC 1566	8.3	6.6	37.3	17	1933	1910	1.50	1300
NGC 1672	6.6	5.5	33.5	15	2001	1352	2.00	1300
NGC 3344	7.1	6.5	23.7	6.9	1930	1908	1.50	1300
NGC 3486	7.1	5.2	42.9	12	1932	1910	1.25	1300
NGC 4303	6.5	5.8	26.8	17	1932	1909	1.25	1300
NGC 4736	11.2	9.1	35.6	5.2	1932	1910	1.65	1300
M83	12.9	11.5	26.9	4.5	935	2456	1.25	1400
NGC 5474	4.8	4.3	26.3	6.8	1938	1900	1.75	1300
NGC 7479	4.1	3.1	40.8	35	1932	1904	1.25	1300

list of 11 galaxies presented in Table 1 and refer to this as our base sample.

We refer the reader to Martin et al. (2005) and Morrissey et al. (2005) for a description of the mission and its on-orbit performance. The images and object catalogs used here are drawn from the database made available by the *GALEX* team via the MAST archive. The archival catalogs contain source positions and photometry in both the FUV (1350–1750 Å) and NUV (1750–2750 Å) channels and were constructed using SExtractor (Bertin & Arnouts 1996). Outside $\sim 1.5R_{25}$ from the centers of the target galaxies, the catalogs appear to faithfully recover nearly all visible sources (see Fig. 1). We discuss this issue in more detail below. The field of view is a circle of 1.2° diameter. The pixel scale is $1.5''$ pixel^{-1}, and the image point-spread function has a FWHM of $4.6''$. Exposure times range from 541 to 4019 s per filter among the galaxies in our sample. The exposure times are equivalent in the two channels for all of our galaxies. Quoted magnitudes are on the AB system and $m = 0$ corresponds to 1.4×10^{-15} and 2.05×10^{-16} ergs s^{-1} cm^{-2} Å^{-1} for the FUV and NUV bands, respectively.

We use the NUV astrometry and aperture photometry to define the object sample, and use the FUV matched aperture photometry to define the FUV − NUV color. Among the set of available apertures, we select the 7 pixel aperture as a compromise between including a significant fraction of the light from the source (7 pixels corresponds to approximately 2 FWHM) and minimizing contamination from nearby sources. These apertures are plotted in Figure 1. We trim the full object catalog for each galaxy using a chosen outer image edge, beyond which the catalogs appear to often have spurious sources, and an inside radius from the target galaxy, within which the catalogs are clearly deficient in detecting sources, perhaps due to source confusion. The outer cut is defined relative to the field-of-view center and occurs typically at a radius of about 1300 pixels. The inner cut is defined relative to the target galaxy nucleus and is typically at a radius of about $1.5R_{25}$. The adopted values for each of these cuts are based on visual inspection of the images and source catalogs and are given in Table 1. An error in the placement of the inner cut will either cause a spurious drop in counts at small radii (if the cut is placed at too small a radius), or preclude us from measuring the correlation function at small radii. An error in the outer radius can affect the knot counting statistics (if the choice does not properly exclude the area with spurious detections), but is clearly identifiable by a nonzero level of the background over a range of radii.

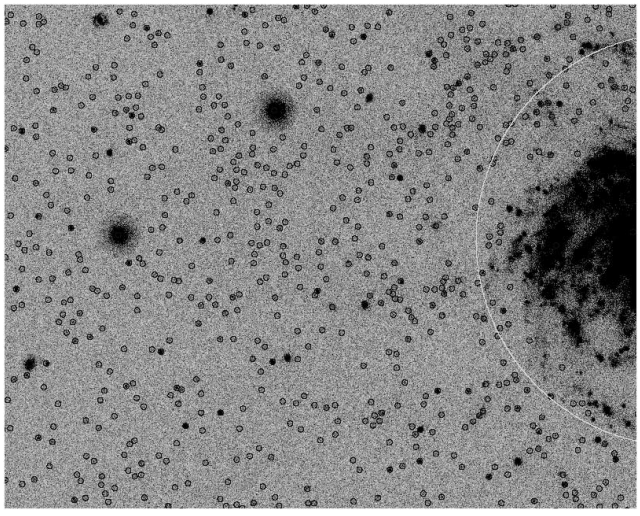

Fig. 1.—Source identification in a subfield around NGC 628. The gray scale represents the *GALEX* NUV image (the subsection is $20'$ across). Small black circles denote detected sources. The large white circle denotes the excluded region in our analysis around NGC 628.

Using the object catalogs, we calculate the angular correlation function, $\xi(r)$, of sources. The correlation function is defined in the standard manner—the excess probability of finding a source at an angular distance r from the reference source. A random distribution of sources, such as that of the background field, will average out to a correlation function of zero at all radii (ignoring exotic effects such as gravitational lensing by the target galaxy or obscuration by galactic dust at large radii; for an example of the effects of the latter at optical wavelengths, see Zaritsky 1994).

Although a natural choice is to use all the objects in the catalog to construct $\xi(r)$, judicious choices can enhance the contrast of the extended disk UV knots to the background population. Previous studies in individual galaxies have stressed the blue UV color of the most evident population of outer disk sources (Thilker et al. 2005; Gil de Paz et al. 2005), so one advantageous possibility is to focus on the bluer of the detected sources. Figure 2 contains the color-magnitude distribution of sources in the NGC 628 field, which is one of the galaxies in the sample for which the extended disk UV knots are most evident. The figure includes both blue and red plumes. The blue plume is where the previous extended disk sources were identified, and we have included labels indicating the corresponding color for single stellar populations at two ages drawn from the modeling of Bianchi et al. (2005). When discussing results below, we refer to the following populations: "all" sources have FUV − NUV < 10 and NUV < 25, "bright blue" sources have FUV − NUV < 1 and NUV < 23, "blue" sources have FUV − NUV < 1 and NUV < 25, "bright red" sources have

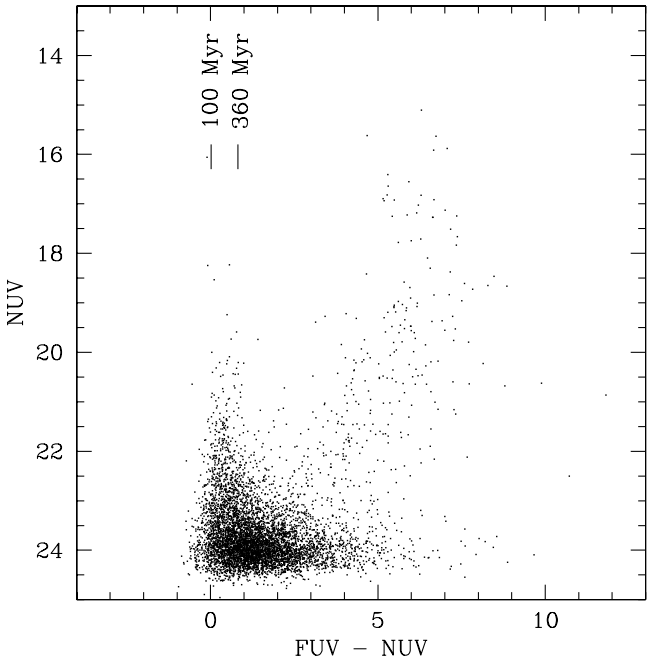

FIG. 2.—Color-magnitude diagram of UV knots. The colors of two single stellar population models of age 100 and 360 Myr are shown from Bianchi et al. (2005).

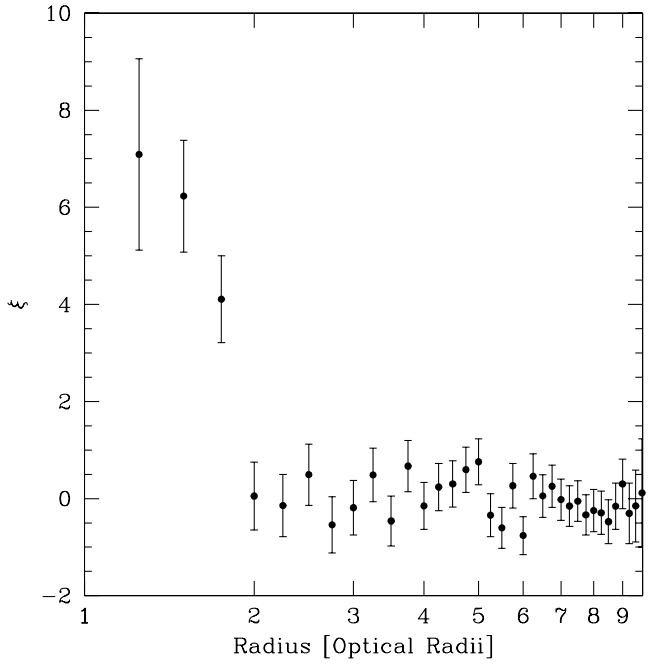

FIG. 3.—Correlation function of blue (FUV − NUV < 1) UV-selected knots for the combined final galaxy sample.

FUV − NUV > 4 and NUV < 23, and "faint red" sources have FUV − NUV > 4 and 23 < NUV.

There are various choices that must be made when calculating $\xi(r)$ from a sample of reference sources, as is the case here. First, the radial coordinate must be defined. The simplest choices are either purely angular (arcseconds) or physical (kiloparsecs), but the galaxies are at different distances and of different intrinsic sizes so neither is an optimal choice. Instead, we use a distance independent scaling radius: optical radii in angular units. With this choice, $\xi(r)$ now describes the excess probability of finding a source at a certain number of optical radii from the central galaxy. Second, the density of sources within different fields, and within a set number of square optical radii, must be considered. To account for field-to-field differences, we calculate $\xi(r)$ in each field first, and then average the individual galaxy values of $\xi(r)$ to obtain the final $\xi(r)$. This approach has the apparent disadvantage that we are not using the entire sample to obtain a highly precise measurement of the mean background, but instead measure the background from each individual image. However, it has the advantage that the measurement of $\xi(r)$ is not dominated by a field with an unusually high background. Within each image, we measure the mean background using source counts at radii $>4R_{25}$, which is the farthest that anyone has yet claimed a detection of UV knots (Gil de Paz et al. 2005). Our initial size criteria have ensured that we have a sample of galaxies for which a single *GALEX* image has significant coverage beyond $4R_{25}$, from which we can measure a background source density. The final values of $\xi(r)$ are expressed as a surface density of objects in units of UV knots, or stellar cluster candidates, per square optical radius.

3. RESULTS

In Figure 3 we present $\xi(r)$ for blue sources. There is a strong signal within $2R_{25}$, and no significant excess of sources thereafter. The flat correlation function beyond $2R_{25}$ argues against certain potential systematic problems and confirms that defining the mean background at radii $>4R_{25}$ is reasonable. The transition in $\xi(r)$ is sharp and probably underrepresented here due to possible increasing incompleteness in the source catalogs toward smaller radii (high source densities). Some incompleteness is suggested by the negative $\xi(r)$ values at small r for the two red samples of objects (Fig. 4), which might be expected to be background objects and therefore uniformly distributed. However,

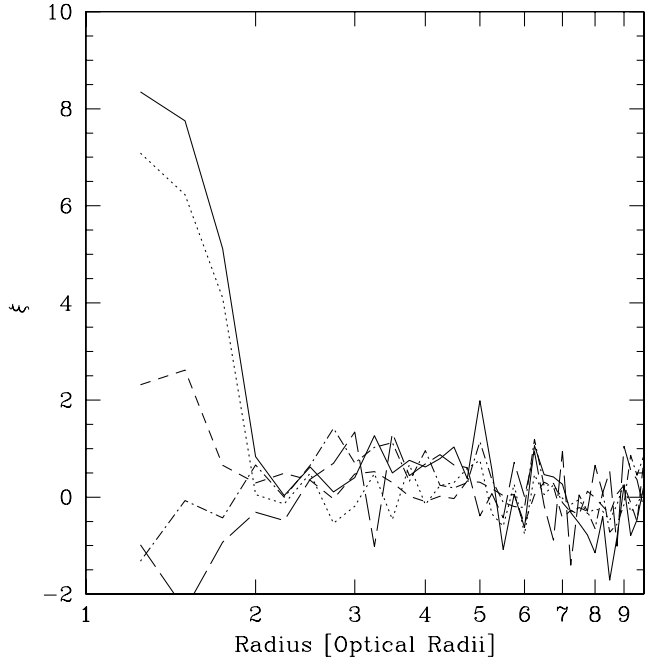

FIG. 4.—Correlation function of UV-selected knots as a function of knot selection parameters: all sources (FUV − NUV < 10, NUV < 25), solid line; blue sample (FUV − NUV < 1 and NUV < 25), dotted line; bright blue sample (FUV − NUV < 1 and NUV < 23), short-dashed line; bright red sample (FUV − NUV > 4 and NUV < 23), long-dashed line; and faint red sample (FUV − NUV > 1 and NUV > 23), dot-dashed line.

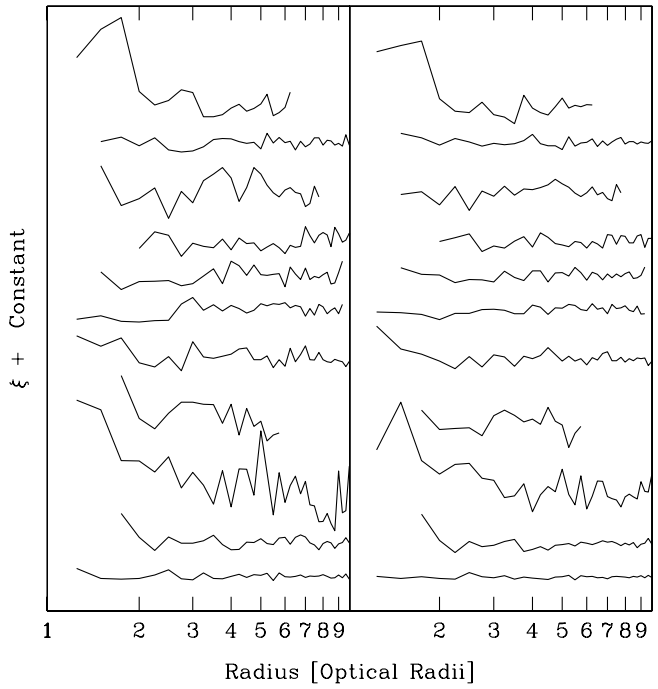

FIG. 5.—Correlation function of UV-selected knots for the individual galaxies. Correlation functions from all sources are shown in the left panel, and only those from the blue sample (FUV − NUV ≤ 1) are shown in the right panel. The correlation functions have been shifted vertically for clarity. The galaxies are in the same order as in Table 1, beginning with NGC 628 at the top of each panel.

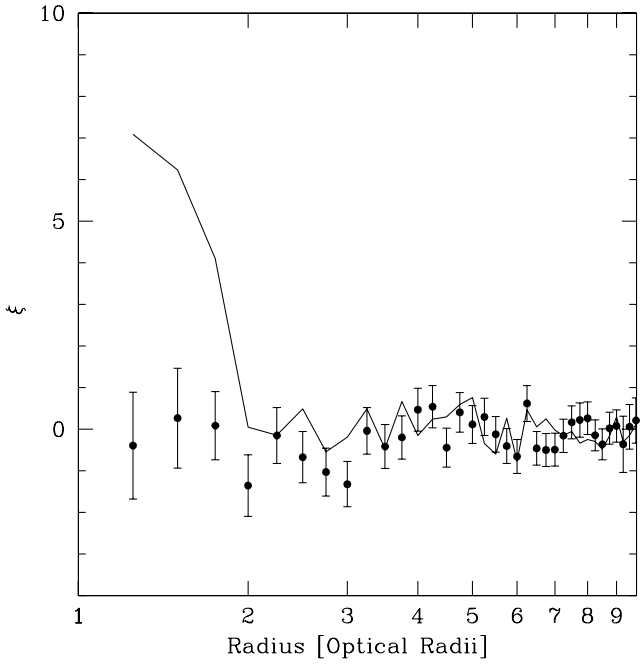

FIG. 6.—Correlation function of UV-selected knots in a selected subsample of galaxies (*circles with error bars*). We removed the galaxies that show the strongest signature of extended disk sources (NGC 628, NGC 4303, NGC 4736, NGC 5474, and M83). The correlation function for the combined sample is the solid line and is shown for comparison.

other explanations for the deficit at small r, such as extinction of background sources (Zaritsky 1994), have not been excluded.

As previously mentioned, the strength and clarity of the correlation function signal may depend on the color of the population. In Figure 4 we plot $\xi(r)$ obtained using all objects and isolating blue, bright blue, bright red, and faint red sources. The strongest signal comes from using all the objects, and there is no signal from either red population. This combination of results suggests that there are some sources with intermediate colors that contribute signal. However, the stronger signal obtained inside of $2R_{25}$ using all sources is countered by a poorer baseline for $\xi(r)$ beyond $2R_{25}$ due to the poorer discrimination of background sources. For this reason, we focus on results using the blue sample.

A key concern in any stacking analysis is whether the final result reflects a universal trend or is dominated by a small subsample of sources. In Figure 5 we plot the correlation functions for each of the 11 galaxies. One of the galaxies, NGC 1672, has no data at $r < 2R_{25}$ and is excluded from further discussion here. Five galaxies show a significant rise in $\xi(r)$ for small r ($r < 2R_{25}$): NGC 628, NGC 4303, NGC 4736, M83, and NGC 5474. We define what is significant here by calculating the number of knots detected in the "all" sample and requiring that this value be sufficiently large that it is statistically unlikely to happen in one galaxy in a sample of 10. In fact, the least significant of these detections (NGC 4736) is likely to happen only 4% of the time by random chance (in other words, we have 96% confidence that our detections of knots in this galaxies is not due to random fluctuations). If we remove these five galaxies from the sample and combine the remainder, we find no significant positive correlation signal within $2R_{25}$ (Fig. 6). The five galaxies for which there is no detected signal are farther on average than those that produce a signal (17.8 vs. 8.9 Mpc), suggesting that we may be less sensitive to the knots and more susceptible to source confusion, although excluding NGC 7479 from the calculation of the distances makes the difference less striking (13.5 vs. 8.9 Mpc). Using binomial statistics, we calculate the smallest intrinsic fraction of galaxies with knots for which there is at least a 10% chance of finding five or more positive detections in a sample of 10. This value is 0.27, so we conclude that with 90% confidence at least 27% of spirals have UV knots at radii between $1.25R_{25}$ and $2R_{25}$.

To examine the possibility that we are missing the UV knots in some galaxies due to their greater distances in more detail, we consider only blue sources (those with an age <360 Myr). The typical uncertainty in the combined $\xi(r)$ for galaxies that show no evidence individually of excess sources (Fig. 6) is $\sim$1 in our units, which suggests that even if $\xi(r)$ was a factor of $\sim$3 lower in these galaxies we would have detected a significant difference from zero in at least the innermost radial bin. The different mean distances of the samples corresponds to a factor of 4 (2.3) in luminosity or 1.5 (0.9) mag, with (without) NGC 7479. In Figure 4 we show that even if we raise the magnitude limit by 2 mag (bright blue vs. blue samples) we retain a positive signal from the entire sample. We conclude that distance alone is not responsible for the lack of a detection of extended disk UV knots in the subsample of five galaxies.

Finally, we examine whether we can enlarge the sample by relaxing some of the selection criteria. Our criteria, which are superposed on whatever criteria were applied by the original observers, are angular size, inclination, and morphological type. The quantitative cuts we adopt for the first two are in some way arbitrary. For example, the need for face-on galaxies does not dictate that one use an inclination value of 45°. Morphological type is the only one of the three for which a change affects the physical character of the sample, and therefore we do not relax that criteria.

We begin by modestly modifying the inclination cut from 45° to 50°. This change increases our sample size from 11 to 17 (adding NGC 1961, 3351, 3368, 6902, 7741, and 7793). Only one of these galaxies individually show a significant rise in the correlation

function at small radii (NGC 6902), where significant is defined as described previously, and the combined correlation function decreases slightly so that the number of knots for the entire sample between $1.25R_{25}$ and $2R_{25}$ declines from 33 ± 5.8 to 19.6 ± 3.8. Although the numbers decline, perhaps because the mean distance of these galaxies is larger than that of the base sample, the significance of the detection of a source excess remains $>5\ \sigma$. Increasing the inclination cut by an additional 10° only increases the sample by 50%. Large gains in sample size cannot be achieved by modest changes in the inclination cut, and the analysis becomes much more ambiguous due to the projection effects.

We now modify the angular size criteria. The primary consideration here is that angular size maps onto distance and distance affects our analysis in two ways. First, the knots of the more distant galaxies are naturally fainter, and hence the data do not reach as far down the luminosity function. This change reduces the number of knots detected significantly. Second, these fewer knots are embedded in a relatively more numerous background (because the intrinsically scarce bright knots are now embedded in the large background population of faint sources). Because selecting galaxies at larger distances reduces both the absolute numbers of detected knots and the contrast, we expect a sharp decrease in our ability to measure a positive correlation function. We have identified a sample of 13 independent galaxies (i.e., not in either the base or inclination-extended sample) that have $2 < a < 4$ and are at distances <50 Mpc. These were winnowed from a sample of 18 that satisfied the same criteria. The rejected galaxies either had bright or multiple companions or there were large-scale problems with the images (variable reddening or scattered light). At 50 Mpc, the brightest of the knots observed in the nearer sample have an apparent magnitude of $\sim$24.5. This sample shows no significant excess (integrated counts from $1.25R_{25}$ to $2R_{25}$ are 0.92 ± 1.65). To detect this value at $6\ \sigma$, comparable to what is done with the base sample, would require a sample that is 115 times larger (i.e., 1500 galaxies). It is therefore not possible with the *GALEX* data set to exploit large numbers to offset the drop in detection sensitivity and relative contrast to the background. We use the results from the base sample in the discussion.

4. DISCUSSION

The identification of extended disks in at least a quarter of disk galaxies indicates that this is not a fringe phenomenon that affects some systems with rare specific histories, such as recent interactions (e.g., M83 and NGC 4625; Kobulnicky & Skillman 1995; Bush & Wilcots 2004). Instead, we conclude that spiral galaxy disks are commonly at least 2 times larger than indicated by their optical radii and that in physical size they can extend out to 26 kpc (2 times the average optical radius, which is 12.9 kpc for this sample). While the average optical radius is 12.9 kpc, the galaxies in the sample radii span from 4.7 to 20.9 kpc. The five galaxies for which we detected correlated signal on an individual basis span the same range, suggesting that this phenomenon is not limited to systems with abnormally large or small optical radii.

Integrating the correlation function between radii of $1.25R_{25}$ and $2R_{25}$ results in a value for the expected excess number of sources of 75 ± 10 knots for galaxies with extended disks (Fig. 7). This number must be treated with some caution because it applies to sources brighter than NUV = 25 for a set of galaxies over a range of distances. If between 5% and 10% of these clusters have associated Hα emission, as suggested in preliminary analysis of observations of knots in NGC 628 (S. Herbert-Fort et al. 2007, in preparation), then a long-slit pointing of an edge-on galaxy should yield between three and seven knots. This expectation is in good agreement with the results of blind slit observations of edge-on galaxies by Christlein & Zaritsky (2007a). This ratio of Hα-emitting sources to nonemitting sources is entirely reasonable given the age estimates of $\sim$20 Myr for H II regions and $\sim$400 for *GALEX* knots (see Fig. 2). Establishing the correspondence between the UV knots and Hα sources is important because we will then be able to connect the kinematics obtained from the Hα observations to the entire population of UV knots. In particular, Christlein & Zaritsky (2007a) have established that the Hα sources follow the disk rotation curve out to $2R_{25}$ and hence lie in a dynamically stable, differentially rotating disk that continues from the inner disk. By inference, the UV knots are also then part of a dynamically cold, extended disk.

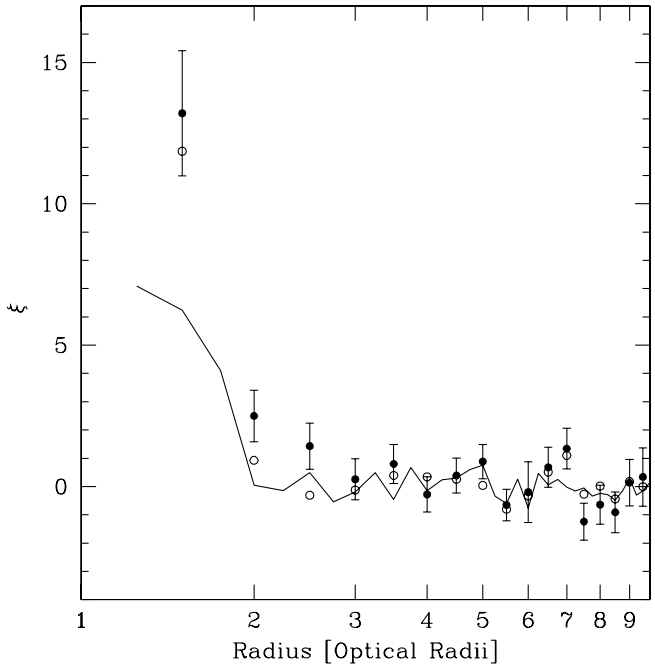

FIG. 7.—Correlation function of UV-selected knots in a selected subsample of galaxies that show the strongest signature of extended disk sources (NGC 628, NGC 4303, NGC 4736, NGC 5474, and M83). The solid line is the composite for the entire sample, and open circles show the results excluding M83.

Connecting the UV knots to other components, for example, H I or dust, will enable further study of the evolution of material at these radii. Thilker et al. (2005) found a general correspondence between H I filamentary structure and UV knots in M83, suggesting that H I could be used to trace the extent of recent star formation in extended disks. We find a correspondence between the radial range over which we find UV knots and that over which 100 μm emission was detected by Nelson et al. (1998). In their most sensitive composite sample, Nelson et al. (1998) found 100 μm emission with $2\ \sigma$ confidence out to $2R_{25}$, exactly the radius out to which we find UV knots. Furthermore, Nelson et al. (1998) show that the emission they detect comes from a disklike component, again consistent with the geometry found here (in combination with the kinematics presented by Christlein & Zaritsky 2007a). Subsequent studies have found more direct evidence for dust in extended disks (Popescu & Tuffs 2003), and the correspondence of dust to these areas of star formation suggests that exotic transport mechanisms from the inner disk are unnecessary.

To determine what the ages, masses, and contribution to the outer disk surface brightness of these knots might be, we have run PEGASE.2 (Fioc & Rocca-Volmerange 1997) models of clusters. Rather than the standard single stellar population models, we vary the length of the burst (modeled by a Gaussian star

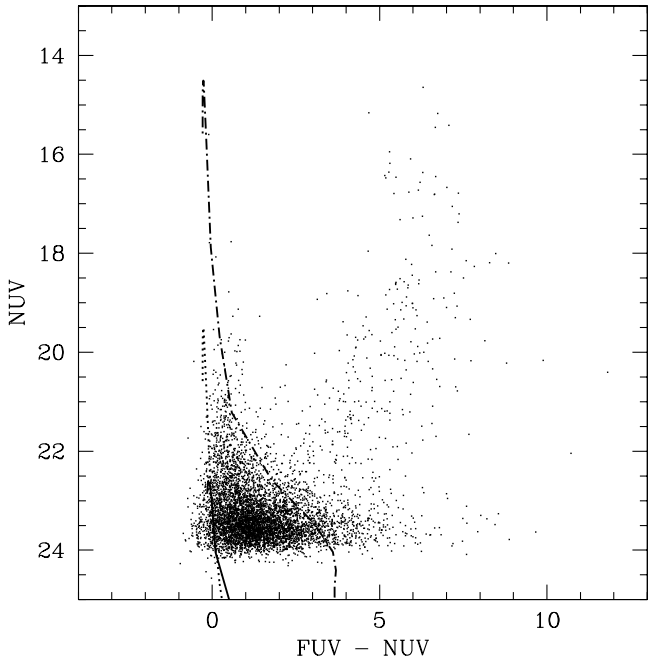

FIG. 8.—Models for the evolution of stellar clusters superposed on properties of observed UV knots in NGC 628 (corrected to a distance of 8.9 Mpc). The solid line represents a cluster with a mass of 1000 $M_\odot$ with a Gaussian burst timescale of 100 Myr, while the dotted line represents the same mass cluster with a burst timescale of 1 Myr. The dot-dashed line represents a 10^6 $M_\odot$ cluster with a burst timescale of 1 Myr. All models are plotted for an assumed distance equal to the mean of the galaxies that show the excess knot population (8.9 Mpc). Models do not include any extinction.

formation rate in time of dispersion, S Myr). We include models with $S = 1$ and 100 Myr in Figure 8. These models are otherwise standard: Salpeter IMF for $0.1\ M_\odot < M < 120\ M_\odot$, and default PEGASE assumptions regarding winds, reprocessing of metals, nebular emission, and extinction. Changes in the initial metallicity or IMF do not produce changes that are sufficiently large to impact the conclusion discussed here. We show models of clusters with total masses of 10^3 and 10^6 $M_\odot$ in Figure 8. The mass of the 10^3 $M_\odot$ cluster is only about a factor of 2 higher than the minimum mass cluster that is likely to have a star with $M > 20\ M_\odot$ (the lowest mass star that will power an H II region), while the upper mass limit appears to represent an upper bound to the likely cluster mass range given the dearth of observed clusters with NUV < 19. With this range of models, and some reddening variations, it appears entirely possible to have simulated clusters fill the entirety of the region in color-magnitude space occupied by the majority of detected sources. The two models with different S values demonstrate the sensitivity of the peak luminosity on the duration of the star formation episode, and signal the difficulty in assigning unique ages or masses to candidates.

We conclude from Figure 8 that the sources in the blue plume are likely to be clusters younger than 400 Myr in the mass range $10^3\ M_\odot < M < 10^6\ M_\odot$, in concurrence with earlier findings by Thilker et al. (2005), Gil de Paz et al. (2005), and Bianchi et al. (2005). If these clusters form uniformly during those 400 Myr (consistent with the rough Hα statistics available), and if 50% of spirals have these populations, then either 50% of spirals have such sources in their outer disks all the time, these sources are generated on timescales of a few hundred megayears in spirals, or something in between. Either alternative, or a combination, indicates that triggering star formation in the outer disk is common. If 50% of spirals have these all the time, and if they typically have 70 such knots between $1.25R_{25}$ and $2R_{25}$, then over the course of 10 Gyr they will have had $70(10/0.4) = 1750$ knots. If these knots have a typical mass of 10^4 $M_\odot$, then the outer disk at these radii contains a stellar mass of $\sim 1.7 \times 10^7$ $M_\odot$. Using the predicted evolution of the V-band magnitude from the models, we integrate (using broad, 1 Gyr time bins, which results in a slight underestimate of the V magnitude) to obtain the V magnitude of these stars currently. For an assumed distance of 8.9 Mpc we find $V \sim 17.5$. For a middle ground value of a of 4′, the area between $1.25R_{25}$ and $2R_{25}$ equals 27,596 arcsec^2, implying an average surface brightness of $\sim$29 mag arcsec^{-2} in V, which is comparable to what the deepest studies reach (although with the expected surface density gradient expected from $1.25R_{25}$ to $2R_{25}$, this population may be easily detectable at $1.25R_{25}$ and nearly impossible to detect near $2R_{25}$). We have ignored reddening due to the low inferred dust content at these radii from both extinction measurements (Zaritsky 1994) and far-infrared luminosity (Nelson et al. 1998). We conclude from our modeling that the observed rate of star formation in the outer disk integrated over a Hubble time does not grossly violate photometric observations of disks, and that in some cases my be consistent with the observed optical surface brightness at large radii (Pohlen et al. 2002; Pohlen & Trujillo 2006). These models are presented simply to begin a discussion of the characteristics of this population and clearly await both tighter observational constraints and more detailed and comprehensive modeling.

5. CONCLUSIONS

We have studied the distribution of UV-selected sources surrounding a sample of nearby, face-on spiral galaxies with the intent of quantifying some properties of the previously discovered population of star-forming regions well beyond the optical radii of these galaxies (Ferguson et al. 1998; Thilker et al. 2005; Gil de Paz et al. 2005; Bianchi et al. 2005). We find the following:

1. Using the cross-correlation function of selected subsamples of UV knots and the primary galaxy, we detect an excess of sources in 50% of our sample for $1.25R_{25} < R < 2R_{25}$. From the integrated counts of knots in this radial range, the detection of knots at extended radius as a general, although not ubiquitous, phenomenon of spiral galaxies is demonstrated at >5 σ significance. We conclude, with 90% confidence, that at least 27% of spirals have such UV-source populations.

2. In the combined data set (11 galaxies), we find no evidence for excess sources beyond $2R_{25}$. Individually, only M83, exhibits an excess of sources beyond $2R_{25}$ (in agreement with Thilker et al. 2005). Therefore, while such star formation is relatively common interior to $2R_{25}$, it is rare beyond.

3. We find the majority of the correlation signal comes from blue sources (FUV − NUV < 1), but that there is detectable signal from redder sources ($1 <$ FUV − NUV), indicating the presence either of some sources older than 400 Myr or reddened sources. If they are older than 400 Myr, then they need to be fairly massive ($M > 10^5$ $M_\odot$). Because of the rapid fading of clusters at UV wavelengths, the prominence of the blue plume does not rule out older clusters, nor suggest the uniqueness of the current episode of cluster formation.

4. The average number of excess blue sources between $1.25R_{25}$ and $2R_{25}$ around spiral galaxies is 33.0 ± 5.8 (75 ± 10 for those galaxies that show a statistically significant excess individually). In combination with the numbers of observed Hα knots (a few in edge-on observations [Christlein & Zaritsky 2007a] and 10% of

UV-selected sources [S. Herbert-Fort et al. 2007, in preparation] in NGC 628), we conclude that the formation rate of these knots could be uniform over the last 0.5 Gyr.

5. Integrating the number of such sources over the lifetime of a galaxy, we obtain an estimate of the average V-band surface brightness of such sources of $\sim$29 mag arcsec^{-2}. Given the expectation of a gradient in surface density, the surface brightness corresponding to these sources may be within relatively easy reach at the inner boundary of the range ($1.25R_{25}$) and nearly impossible at the outer edge ($2R_{25}$). The simple calculation suggests that the extended disks seen in diffuse light in many galaxies (Pohlen et al. 2002; Pohlen & Trujillo 2006) could arise from a long-term population of evolved UV knots.

The outer, or extended, disk environment is well populated by recently ($t < 400$ Myr) formed stellar clusters in a large fraction of disk galaxies. As such, it opens several interesting avenues for study, ranging from the physics of star formation in metal-poor, low-density environments (see, e.g., Boissier et al. 2007), to their use as kinematic tracers in the disk-halo interface. These clusters are a common feature of spiral disks and demonstrate that the stellar disks of galaxies are often twice as large as indicated by the central, high surface brightness disk.

D. Z. acknowledges that this research was supported in part by the National Science Foundation under grant PHY99-07949 during his visit to KITP, a Guggenheim fellowship, generous support from the NYU Physics department and Center for Cosmology and Particle Physics during his sabbatical there, NASA LTSA grant 04-0000-0041, NSF AST 03-07482, and the David and Lucile Packard Foundation. D. C. gratefully acknowledges financial support from the Fundación Andes. The authors thank the *GALEX* team for their work on the satellite, instrument, and data products, without which this study would not have been possible, and the MAST team at STScI for their work in making such data easily accessible to all.

REFERENCES

Bertin, E., & Arnouts, S. 1996, A&AS, 117, 393
Bianchi, L., et al. 2005, ApJ, 619, L71
Boissier, S., et al. 2007, ApJS, in press
Braine, J., & Herpin, F. 2004, Nature, 432, 369
Bush, S. J., & Wilcots, E. M. 2004, AJ, 128, 2789
Christlein, D., & Zaritsky, D. 2007a, ApJ, submitted
de Vaucouleurs, G., de Vaucouleurs, A., Corwin, H. G., Jr., Buta, R. J., Paturel, G., & Fouque, P. 1991, Third Reference Catalogue of Bright Galaxies (Berlin: Springer)
Ferguson, A. M. N., Wyse, R. F. G., Gallagher, J. S., & Hunter, D. A. 1998, ApJ, 506, L19
Fioc, M., & Rocca-Volmerange, B. 1997, A&A, 326, 950
Gil de Paz, A., et al. 2005, ApJ, 627, L29
———. 2006, preprint (astro-ph/0606440)
Kennicutt, R. C., Jr. 1989, ApJ, 344, 685
Kobulnicky, H. A., & Skillman, E. D. 1995, ApJ, 454, L121
Martin, D. C., et al. 2005, ApJ, 619, L1
Morrissey, P., et al. 2005, ApJ, 619, L7
Nelson, A. E., Zaritsky, D., & Cutri, R. M. 1998, AJ, 115, 2273
Pohlen, M., Dettmar, R.-J., Lütticke, R., & Aronica, G. 2002, A&A, 392, 807
Pohlen, M., & Trujillo, I. 2006, A&A, 454, 759
Popescu, C. C., & Tuffs, R. J. 2003, A&A, 410, L21
Roberts, M. S., & Haynes, M. P. 1994, ARA&A, 32, 115
Thilker, D. A., et al. 2005, ApJ, 619, L79
van der Kruit, P. C., & Searle, L. 1981, A&A, 95, 105
Zaritsky, D. 1994, AJ, 108, 1619
Zaritsky, D., Smith, R., Frenk, C., & White, S. D. M. 1993, ApJ, 405, 464